Effect of sputtering time on Mo thin films deposited on different substrates using DC magnetron sputtering

TING-TING LIANG[a], AI-QIN WANG[a,*], HAI-LI ZHAO[b], JING-PEI XIE[c]
[a]*Henan University of Science and Technology, Luoyang, Henan province, 471023, China*
[b]*Zhengzhou University, Zhengzhou, Henan province, 450000, China*
[c]*Collaborative Innovation Center of Nonferrous Metals, Henan province, 471000, China*

Mo thin films were deposited on glass and silicon substrates using DC magnetron sputtering at different sputtering time respectively. Their morphological, structural and electrical properties were investigated. The results show that Mo films present crystal plane orientation along (110) direction. And the grain sizes increase with the increase of sputtering time. In addition, the sheet resistance and resistivity of Mo films show a first decrease and then increase relationship with the increase of sputtering time. Particularly, when the sputtering time is 25 min, the resistivity of Mo film deposited on glass is lowest in this experiment, 12.33 μΩ•cm.

(Received December 5, 2016; accepted October 10, 2017)

Keywords: Mo thin films, Sputtering time, Substrates, Properties

1. Introduction

Nowadays, the researches of thin-film solar cells become more and more popular today [1-4]. Mo thin films have been used widely as batteries back contact layer in thin-film solar cells [5-8] and electrode [9,10] because of their high electrical conductivity, thermal stability, chemical stability and infrared reflection characteristics [11-13]. Besides, Mo films are also widely used as gate and source/drain signal lines in the thin film transistor-liquid crystal displays (TFT-LCD) or as interconnection lines in resistive and capacitive touch screen panels owing to their excellent adhesion property on glass substrate and low contact resistance to silicon and indium tin oxide (ITO) [14]. High conductivity and uniformity, low sheet resistance and commensurate thermal expansion coefficient of Mo thin films are most essential characteristics in application [15].

So far, many scholars have devoted to explore the preparation and properties of Mo thin films by sputtering method [16-20]. Different parameters of sputtering process will effect the microstructure and performance of thin films such as the power, current, temperature, Ar pressure and base pressure [21-24]. Besides, sputtering time and the properties of the substrates also can effect the microstructure and performance of Mo thin films. Hence, Zhang et al. [25] have studied the influence of sputtering time on the preferred orientations of Mo thin films. And Tanja et al. [26] studied the electro-mechanical behavior of Mo thin films deposited on flexible substrates. But all of the works mentioned above were focused on the influence of one single parameter in sputtering process. To study more comprehensively about the effect of sputtering process on Mo thin films, we paid great attentions on the difference in microstructure and properties of Mo thin films deposited on different substrates at different sputtering time using DC magnetron sputtering method, respectively.

2. Experimental

Mo thin films were deposited on 10 × 10 mm^2 soda-lime glass and mono-crystalline silicon substrates with 1.0 mm thickness using DC (direct current) magnetron sputtering at room temperature. The Mo target was a disc of 25 mm diameter, 4 mm thickness with 99.97% purity. And the distance between target and substrates was 60 mm. The substrates were cleaned by acetone, alcohol and deionized water using a ultrasonic cleaners for 15 min respectively in order to remove impurities and contaminants. Then the substrates were dried in N_2 atmosphere prior to deposition. The cleaned substrates were transferred to the deposition chamber immediately after drying. Prior to each deposition, pre-sputtering of target was performed for 10 min to remove impurities from the surface of target. The parameters of sputtering process are shown in Table 1.

Table 1. Summary of conditions of Mo thin films deposited by DC magnetron sputtering

Samples	Base pressure/Pa	Power/W	Current/A	Working pressure/Pa	Ar flow/sccm	Sputtering time/min
1	2×10^{-5}	110	0.25	0.35	40	8
2	2×10^{-5}	110	0.25	0.35	40	10
3	2×10^{-5}	110	0.25	0.35	40	15
4	2×10^{-5}	110	0.25	0.35	40	25
5	2×10^{-5}	110	0.25	0.35	40	35

The morphologies of Mo thin films were observed using scanning electron microscope (SEM) and the phase structure of the Mo thin films were determined by X-ray diffraction (XRD). Besides, the sheet resistance was measured by a four-point probe equipment. And then the resistivity of the samples was calculated combining with the thickness by the formula (1) following:

$$\text{Resistivity} = \text{Thickness} \times \text{Resistance} \qquad (1)$$

Besides, the average crystallite size was calculated by Scherrer equation according to the XRD data. The Scherrer equation can be written as:

$$d=K\lambda/\beta\cos\theta \qquad (2)$$

where: d is the mean size of the ordered (crystalline) domains, which may be smaller or equal to the grain size; K is a dimensionless shape factor, with a value close to unity. The shape factor has a typical value of about 0.9, but varies with the actual shape of the crystalline; λ is the X-ray wavelength; β is the line broadening at half the maximum intensity (FWHM), after subtracting the instrumental line broadening, in radians. This quantity is also sometimes denoted as $\Delta(2\theta)$; θ is the Bragg angle.

Furthermore, the shift of the (110) peak along 2θ allowed us to calculate strain in thin films. The residual stress calculations were made from the XRD data by strain equation. Using Bragg's formula the inter-planar spacing d_{110} was calculated. The strain in the films was then calculated by the formula (3) following:

$$\text{Strain } (\%) = \Delta\alpha/\alpha \times 100\% \qquad (3)$$

where: a is lattice constant(for Mo thin film, a=0.31472 nm). It is the main parameter to determine whether the strain is compressive or tensile [27].

3. Results and discussions

Fig. 1 shows the SEM images of Mo films deposited on silicon substrates. The morphologies of Mo films are significantly effected by the increase of sputtering time. When the sputtering time is short, such as 8min and 10 min, non-uniform grains in the dimension of 20-30 nm are observed resulting in rather rough surfaces as shown in Fig. 1(a, b). When an elevated sputtering time of 15 min is available, more compact and smooth surface is achieved, and the distribution of grain sizes is more homogeneous. As the sputtering time increases to 25 min, most smooth surface is obtained comparing with the others. However, when the sputtering time increases to 35 min, the shape of grains changes from cone into spherical obviously. And some small holes appear in Fig. 1(e). Furthermore, the grain sizes evidently increase with the increase of sputtering time.

The morphologies of Mo thin films deposited on glass substrate are demonstrated by SEM images as shown in Fig. 2. It is obvious that the grain sizes of Mo thin films deposited on the glass substrates increase with the increase of sputtering time. When the sputtering time is less than 15 min, some particles aggregate as shown in Fig. 2(a-c). Because there is not enough energy for the grains to migrate owing to short sputtering time. And then when the sputtering time increases to 25 min, the surface of Mo thin film is most smooth with most uniform grain size in Fig. 2. Besides, the density of Mo thin film shown in Fig. 2(d) is also the highest. However, over long sputtering time results in bigger grain size leading to nonuniform surface and lower density.

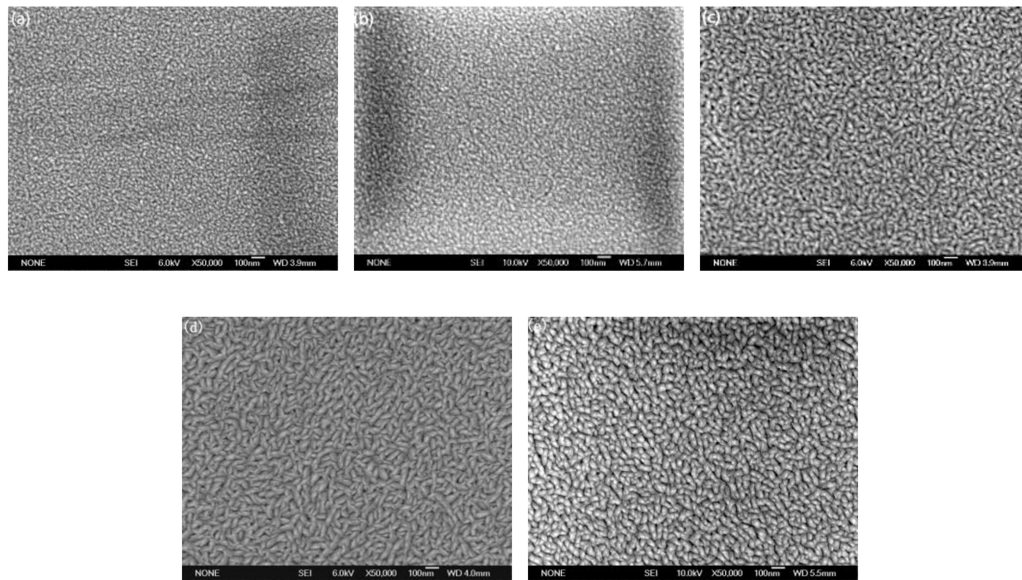

Fig. 1. SEM images of Mo thin films deposited on silicon substrates at different sputtering time: (a) 8 min, (b) 10 min, (c) 15 min, (d) 25 min, (e) 35 min

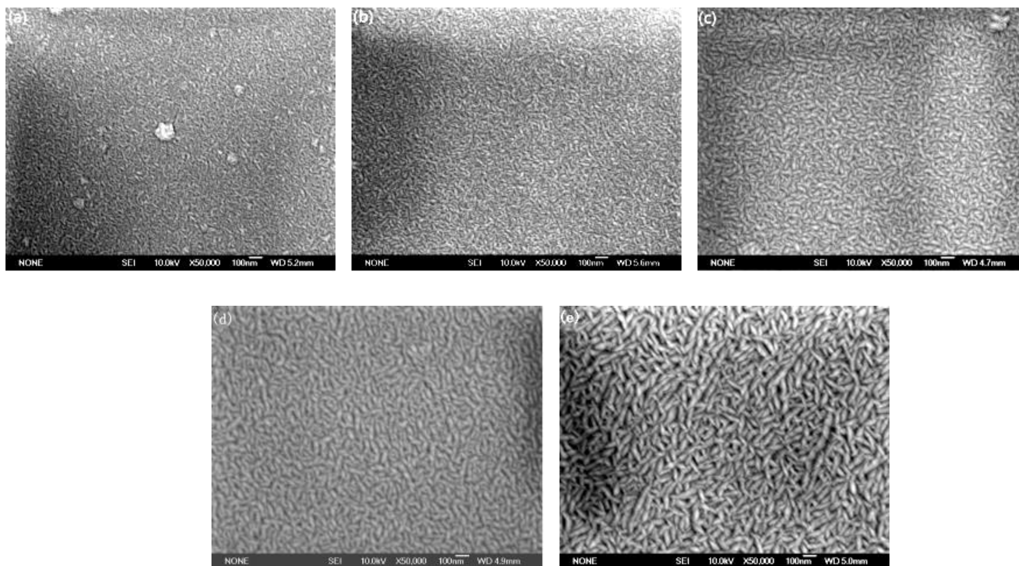

Fig. 2. SEM images of Mo thin films deposited on soda-lime glass substrates at different sputtering time: (a) 8 min, (b) 10 min, (c) 15 min, (d) 25 min, (e) 35 min

Comparing Fig. 2 with Fig. 1 comprehensively, the grain sizes of Mo films deposited on glass are smaller than those of Mo films deposited on silicon substrates at the same sputtering time. It is because that silicon substrate with high crystalline orientation along (400) direction is used in this work. As shown in Fig. 4(a), the XRD data of silicon substrates can be indexed to a pure cubic structure according to JCPDS card No. 65-1060, with space group Fd-3m(no. 227) and lattice parameters of a = b = c = 5.43Å. In addition, the peaks of Mo can be indexed to a pure cubic structure according to JCPDS card No. 65-7442, with space group Im-3m(no. 229) and lattice parameters of a = b = c = 3.147Å. Thus, for silicon substrate, the lattice mismatch (δ) between silicon and Mo is calculated as 0.42 according to the formula (4).

$$\delta = (\alpha_\alpha - \alpha_\beta) / \alpha_\alpha \tag{4}$$

Therefore, the incoherent interface is formed between silicon and Mo grains because the large lattice mismatch resulting in larger phase difference among grains. Thus, the the interface energy is higher. As it is known, the greater the interface energy is, the more unstable the grain boundary is. And then the rate of the atomic migration is higher. It is conducive to the nucleation and growth for grains. As a result, the grain size of Mo thin films

deposited on silicon substrate is larger. Besides, regardless of the influence of substrates, different sputtering time also effects the grain size, morphology, and properties of Mo films. When the sputtering time is 25 min, Mo films present most homogeneous grain size and most smooth surface, which leads to lowest resistivity in this work.

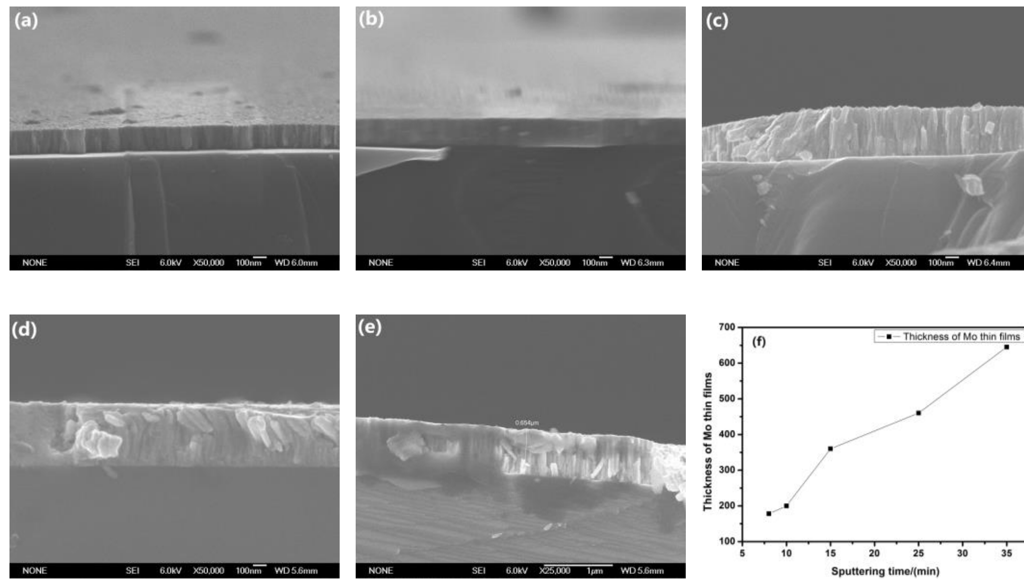

Fig. 3. Cross-section of Mo thin films deposited at different sputtering time: (a) 8min, (b) 10min, (c) 15min, (d) 25min, (e) 35min, (f) thickness of Mo thin films

Fig. 3(a-e) shows the cross-sectional SEM images of Mo thin films deposited at different sputtering time. The Mo grains grow in a columnar crystal growth way as shown in Fig. 3. Moreover, the thickness of Mo thin films shows a linear increasing relationship with the increase of sputtering time approximately as shown in Fig. 3(f). Crystallite sizes and strains of deposited Mo thin films calculated from XRD data are shown in Table 2. Here the crystallite size just means the crystallite property of deposited Mo thin films. In addition, as a reason for the adhesion property, the residual stress is considered. Thus, the residual stress analysis has become meanwhile a mandatory experimental technique for the study of the Mo thin films for electronic applications [28]. In this work, all the Mo thin films show a small tensile. The adhesion properties of Mo films could meet the requirements on use. It has been suggested that voids, crystallographic flaws, argon impurities could be responsible for the stress in the deposited Mo thin films using DC magnetron sputtering method.

Table 2. Crystallite size and strain calculated from XRD data

Sample	1	2	3	4	5	6	7	8	9	10
Substrates	glass	glass	glass	glass	glass	silicon	silicon	silicon	silicon	silicon
Sputtering time(min)	8	10	15	25	35	8	10	15	25	35
Crystallite size(nm)	11.3	16.5	12.0	12.6	20.3	25.5	12.7	16.7	17.1	5.6
Strain,%	0.9182	0.6049	0.8288	0.7884	0.4925	0.2383	0.7725	0.5916	0.6156	1.7701

The XRD patterns of Mo thin films deposited on silicon and glass substrates are shown in Fig. 4. All the Mo films deposited shows cubic crystal structure according to JCPDS card No. 65-7442. No diffraction peaks from any other impurities were observed, indicating the high purity of the products. And Mo thin films deposited on both the Si and the glass substrates exhibit a strong preferential diffraction peak (110). And the intensity of the peak (110) increases with the increasing of sputtering time. However, the intensity of the diffraction peak (110) shown in Fig. 4(b) is higher than Fig. 4(a). It is mainly because of the strong preferential orientation of silicon substrates, which could effect the interface between the substrate and Mo grains as discussed above.

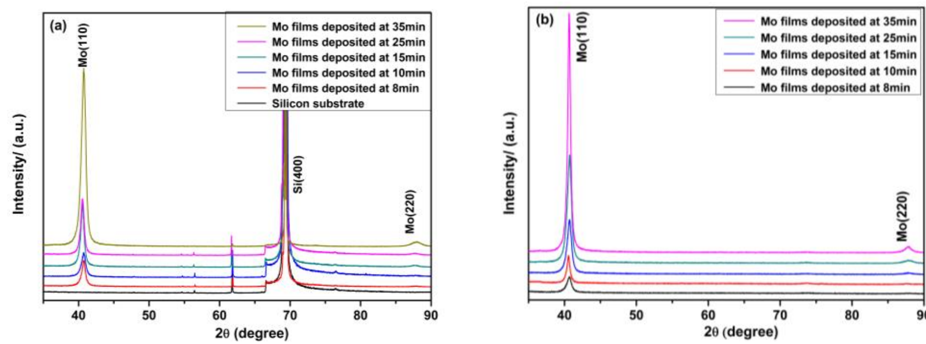

Fig. 4. XRD patterns of Mo thin films deposited on silicon and glass substrates respectively: (a) silicon substrates; (b) glass substrates

Table 3. Electrical properties of Mo thin films deposited on different substrates

Sample	1	2	3	4	5	6	7	8	9	10
Substrates	glass	glass	glass	glass	glass	silicon	silicon	silicon	silicon	silicon
Sputtering time(min)	8	10	15	25	35	8	10	15	25	35
Thickness(nm)	178	200	380	460	645	178	200	380	460	645
Sheet resistance(Ω/sq)	16.82	16.46	6.11	2.68	4.12	25.82	23.18	9.13	4.32	6.00
Resistivity(μΩ•cm)	29.94	32.92	23.24	12.33	26.57	45.96	46.36	34.69	19.87	38.70

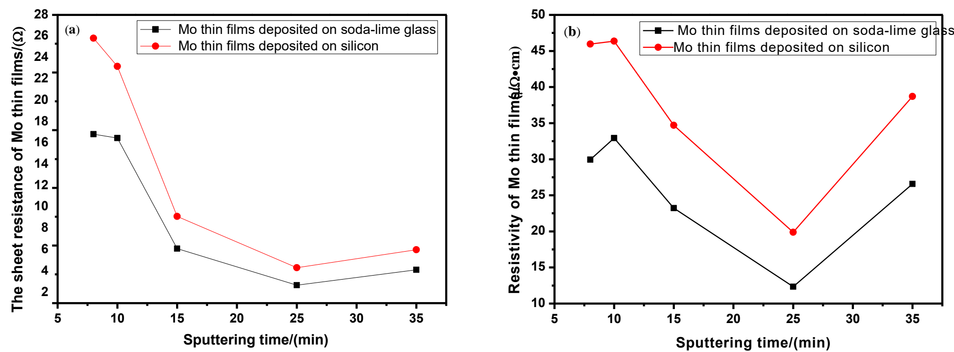

Fig. 5. The sheet resistance and resistivity of Mo films deposited on silicon and glass substrates respectively: (a) sheet resistance, (b) resistivity

Table 3 summarizes the electrical properties of Mo thin films deposited on silicon and glass substrates respectively. Also changes in the sheet resistance and the resistivity of deposited Mo thin films are shown in Fig. 5. It is clear that both the sheet resistances and the resistivity of deposited Mo thin films show a first decrease and then increase relationship with the increase of sputtering time. In addition, it is worth noting that both the sheet resistance and the resistivity of Mo thin films deposited on glass substrates are lower than those of films deposited on silicon substrates at the same sputtering time. As for the films, their resistances are consisted of two parts: resistances at interface and grain boundary. A relationship between numbers of grain and resistance is established by Tamaki et al., which state that resistance is directly proportional to the number of grains as shown in formula (5) [29].

$$Ra = 2Ra(i) + (N-1)Ra(gb) \quad (5)$$

Where, Ra(i) and Ra(gb) are resistance at interface and grain boundary, respectively, and N is the number of grains. For silicon substrates, the incoherent interface is formed between silicon and Mo grains, the interface energy is higher than strain energy, so the Mo films are always formed into spherical phase as shown in Fig. 1. And the crystal sizes of Mo grains deposited on silicon substrate are almost similar as those on glass substrate. In the case, the numbers of grain boundaries are higher for Mo grains deposited on silicon substrate as compared to Mo grains

deposited on glass substrate. As a result, the resistivity of molybdenum films deposited on silicon substrate is higher according to formula (5).

4. Conclusion

We have investigated the effects of sputtering time on the microstructure, sheet resistance and resistivity of Mo thin films deposited on different substrates at different sputtering time in this work. The grain sizes of the Mo thin films deposited on both the glass substrates and silicon substrates increase with the increase of sputtering time. And all deposited Mo films exhibit a strong preferential diffraction peak (110). Moreover, the sheet resistances and the resistivity of deposited Mo thin films show a first decrease and then increase relationship with the increase of sputtering time. In addition, both the sheet resistances and the resistivity of Mo thin films deposited on glass substrates are lower than those of films deposited on silicon substrates at the same sputtering time. Especially, when the sputtering time is 25 min, the resistivity of Mo thin film deposited on soda-lime glass declines obviously to the lowest in this experiment (12.33 μΩ•cm).

References

[1] Sanjay R. Dhage, Hak-Sung Kim, H. Thomas Hahn, J. Electron. Mater. **40**(2), 122 (2011).

[2] Hyeonwook Park, Sung Cheol Kim, Sang-Hwan Lee et al. Thin Solid Films **519**(21), 7245 (2011).

[3] Zhou Yu, Yong Yan, Sha-sha Li et al., Appl. Surf. Sci. **264**, 197 (2013).

[4] J. A. Frantz, R. Y. Bekele, V. Q. Nguyen et al., Thin Solid Films **519**, 7763 (2011).

[5] P. Jackson, D. Hariskos, E. Lotter et al. Progress in photovoltaics: Research and Applications **19**(7), 894 (2011).

[6] Ji-Guo Zhu, Wei-Ping Chai, Hua-Lin Wang et al., Optical Instruments **30**, 55 (2008).

[7] Ju-Heon Yoona, Sunghun Cho, Won Mok Kim et al., Sol. Energy Mater. Sol. Cells **95**(8), 2959 (2011).

[8] Bei-Bei Guo, Yao-Ming Wang, Xiao-Long Zhu et al., Chinese Optics Letters **91**, 043101 (2016).

[9] Xiang-Quan Jiao, Jie Yang, Rui Zhang et al., Mater. Lett. **124**, 318 (2014).

[10] Bao-Hua Zhao, Hai-Bo Fan, Jun-Yuan Sun. China molybdenum industry **35**, 7 (2011).

[11] A. A. Kadam, A. H. Jahagirdar, N. G Dhere. Proceeding of the materials research society spring meeting 423 (2005).

[12] J. H. Scofield, A. Duda, D. Albin et al., Thin Solid Films **260**, 26 (1995).

[13] K. Aryal, H. Khatri, R. W. Collins et al., International Journal of Photoenergy **2012**, (2012).

[14] D. Rafaja, H. Kostenbauer, U. Muble et al., Thin Solid Films **528**, 42 (2013).

[15] K. Orgassa, H. W. Schock, J. H. Werne, Thin Solid Films **431**, 387 (2003).

[16] Yong Yan, Fan Jiang, Lian Liu et al., **12**, 59 (2016).

[17] Zhi-Ming Zhao, Yu Ding, Zhi-Rui Cao et al. Materials guides **25**, 74 (2011).

[18] A. Marcelli, B. Spataro, S. Sarti et al., Surf. Coating Technol. **261**, 391 (2015).

[19] S. Bini, B. Spataro, A. Marcelli et al., Chinese Physics C **37**, 7905 (2013).

[20] Y. Xu, B. Spataro, S. Sarti et al. Journal of Physics: Conference Series **430**(conference 1), 91 (2013).

[21] Abd El-Hady B. Kashyout, Hesham M. A. Soliman, Hanaa Abou Gabal et al., Alexandria Engineering Journal **50**(1), 57 (2011).

[22] Majid Khan, Mohammad Islam, Semiconductors **47**(12), 1610 (2013).

[23] Xin-yi Dai, Ai-jun Zhou, Lin-dong Feng et al., Thin Solid Films **567**, 64 (2014).

[24] M. Jubault, L. Ribeaucourt, E. Chassaing et al., Sol. Energy Mater. Sol. Cells **95**(Supplement 1), S26 (2011).

[25] Xia-Yan Zhang, Xin-Ya Ji, Feng-Yu Ou et al., Functional Materials **44**, 888 (2013).

[26] Tanja Jörg, Megan J. Cordill, Robert Franz et al., Thin Solid Films **606**, 45 (2016).

[27] Jie Xiong, Wen-feng Qin, Xu-mei Cui et al. Physica C: Superconductivity **442**, 124 (2006).

[28] S. S. Wang, C. Y. Hsu, F. J. Shiou et al., J. Electron. Mater. **42**(1), 71 (2013).

[29] J. Tamaki, A. Miyaji, J. Makinodan, S. Ogura, Konishi, S. Sens. Actuators B Chem. **108**(1-2), 202 (2005).

*Corresponding author: aiqin_wang888@163.com